Cell Fate Control Gene Therapy Based on Engineered Variants of Human Deoxycytidine Kinase

Anton Neschadim[1], James CM Wang[2], Takeya Sato[3], Daniel H Fowler[4], Arnon Lavie[5] and Jeffrey A Medin[1,2,6]

[1]Department of Medical Biophysics, University of Toronto, Toronto, Ontario, Canada; [2]Institute of Medical Science, University of Toronto, Toronto, Ontario, Canada; [3]Molecular Pharmacology, Tohoku University, Sendai, Japan; [4]Experimental Transplantation and Immunology Branch, National Cancer Institute, National Institutes of Health, Bethesda, Maryland, USA; [5]Biochemistry and Molecular Genetics, University of Illinois at Chicago, Chicago, Illinois, USA; [6]University Health Network, Toronto, Ontario, Canada

The safety of cell therapy applications can be enhanced by the introduction of Cell Fate Control (CFC) elements, which encode pharmacologically controlled cellular suicide switches. CFC Gene Therapy (CFCGT) offers the possibility of establishing control over gene-modified cells (GMCs) with regards to their proliferation, differentiation, or function. However, enzymes commonly employed in these approaches often possess poor kinetics and high immunogenicity. We describe a novel CFCGT system based on engineered variants of human deoxyCytidine Kinase (dCK) that overcomes limitations of current modalities. Mutants of dCK with rationally designed active sites that make them thymidine-activating were stably introduced into cells by recombinant lentiviral vectors (LVs). Transduced cells maintained growth kinetics and function. These dCK mutants efficiently activate bromovinyl-deoxyuridine (BVdU), L-deoxythymidine (LdT), and L-deoxyuridine (LdU), which are otherwise not toxic to wild-type cells. We show that mutant dCK-expressing Jurkat, Molt-4, and U87mg cells could be efficiently eliminated *in vitro* and in xenogeneic leukemia and tumor models *in vivo*. We also describe a fusion construct of the thymidine-activating dCK to the cytoplasmic tail-truncated LNGFR molecule and applications to *in vivo* eradication of primary human T cells. This novel CFCGT system offers unique plasticity with respect to the wide range of prodrugs it can potentiate, and can be used as a reliable safety switch in cell and gene therapy.

Received 29 March 2011; accepted 16 December 2011; advance online publication 24 January 2012. doi:10.1038/mt.2011.298

INTRODUCTION

The safety of cell therapies in general can be compromised by the *ex vivo* manipulation of the transplanted cells or by the mere placement outside of their natural context *in vivo*. As a result, adverse events can range from graft-versus-host disease (GvHD)[1] to donor cell-derived leukemias[2] to the development of brain tumors[3] in treated patients. Moreover, deleterious complications from cell therapy can even manifest more than a decade following the initial treatment.[4] This reality warrants the development and application of methods that can offer a universal and reliable safety net for cell therapy-based approaches that would endure long term. A solution is offered by Cell Fate Control Gene Therapy (CFCGT), which aims to establish permanent pharmacological controls over the proliferation, differentiation, and/or function of gene-modified cells (GMCs). Transplanted cells, engineered to express such a Cell Fate Control (CFC) element, could then be selectively deleted *in vivo* by the specific activation of an otherwise nontoxic prodrug in such cells.

Historically, the most commonly employed CFCGT strategy relies on the stable delivery of the herpes simplex virus-derived thymidine kinase sequence, which renders transduced cells sensitive to ganciclovir or acyclovir.[5] While clinical studies performed to date have documented the utility of this system, they have also highlighted several limitations of this approach.[6–9] This modality is suboptimal due to poor prodrug activation kinetics,[10–12] escape from drug selection,[7,13–15] and immunological rejection of GMCs due to the foreign nature of the transgene product.[16,17] The widespread reliance on prophylactic ganciclovir to control opportunistic cytomegalovirus infections in patients undergoing transplantation further limits the broad implementation of herpes simplex virus-derived thymidine kinase-based CFCGT.[18]

We have previously described a novel CFCGT strategy based on the lentiviral delivery of a thymidylate monophosphate kinase variant that potentiates the activation of the prodrug azidothymidine.[19] While this system overcomes some of the major limitations of currently employed approaches, we sought to develop additional CFCGT strategies to improve and possibly complement our thymidylate monophosphate kinase/azidothymidine axis. Firstly, we sought an enzyme-prodrug system that would act earlier in the prodrug activation pathway enabling the rapid accumulation of the active metabolites in the cells. Secondly, we sought an enzyme that overcomes the rate-limiting step in the activation pathway of its substrates. And, thirdly, we sought a system that has the

Correspondence: *Jeffrey A Medin, University Health Network, 67 College Street, 4th Floor, Room 406, Toronto, Ontario M5G 2M1, Canada. E-mail: jmedin@uhnres.utoronto.ca*

potential capacity for tracking therapeutic progress in a clinically applicable manner.

We now describe a next-generation CFCGT strategy based on active site-engineered variants of the human deoxyCytidine Kinase (dCK) enzyme. This enzyme is an essential kinase in the salvage pathway of nucleotide synthesis. dCK normally catalyzes the monophosphorylation of deoxyadenosine, deoxyguanosine, and deoxycytidine nucleosides, but not deoxythymidine or deoxyuridine. Activation of a multitude of nucleoside analogue-based prodrugs is mediated by dCK, and it is also capable of phosphorylating nucleosides with the nonphysiological L-chirality.[20–22] The determination of the X-ray crystal structures of this enzyme in complex with different substrates facilitated the rational modification of its active site to improve the catalytic efficiency and alter substrate specificity.[23] In one embodiment, human dCK was modified to generate the dCK.R104M.D133A double mutant that accommodates deoxythymidine and deoxyuridine nucleoside analogs (NAs) at its active site.[24] Phosphorylation of several well-characterized prodrugs, such as bromovinyl-deoxyuridine (brivudine or BVdU), L-deoxythymidine (LdT), and L-deoxyuridine (LdU) is catalyzed by this thymidine-activating mutant of dCK with high efficiency (kcat/K_m of 1.0–2.3 × 10^4 l/mol s^{-1}).[25] The nucleoside kinase activity of dCK is further regulated in the cell by phosphorylation of the Ser74 residue, and mimicking this phosphorylation by a S74E mutation was shown to dramatically increase dCK activity—up to 11-fold.[26,27] Furthermore, dCK is the rate-limiting enzyme in the phosphorylation pathway of nucleosides in the cell.[28] Lastly, the ability of these dCK mutants to facilitate rapid retention of thymidine-based radiotracers also provides capabilities for direct imaging of GMCs *in situ* by positron emission tomography.[29]

Here, we report that stable recombinant lentiviral vector (LV)-mediated delivery of dCK.R104M.D133A (dCK.DM, for double mutant), dCK.R104M.D133A.S74E (dCK.DM.S74E), and dCK.DM.S74E fused to truncated LNGFR renders human cells highly sensitive to the prodrugs BVdU, LdT, and LdU via induction of apoptosis. We further demonstrate that our mutant dCK-based CFCGT is highly selective for cells expressing the thymidine-activating mutants of dCK, but not for cells overexpressing wild-type dCK. We also show that the mutant dCK/BVdU-based CFCGT induces apoptosis via an additional pathway that is distinct from the incorporation of the cytotoxic BVdU metabolites into newly synthesized DNA. This pathway allows for cell cycle-independent killing of nondividing cells via BVdU activation. Finally, we demonstrate the utility of the dCK-based CFCGT in stringent murine models of xenogeneic tumors and aggressive leukemias *in vivo*. These dCK mutants thus provide for robust activation and accumulation of a multitude of NA-based prodrugs, overcome the rate-limiting prodrug activation step, and act early in the activation pathway enabling rapid accumulation of activated NAs in target cells.

RESULTS

Construction and validation of novel LVs for dCK-based CFCGT

The constructs developed in this study for the lentivirus-mediated delivery of engineered human dCK variants are diagrammed in **Figure 1a**. We used a bicistronic design we have employed previously.[19] For initial studies, we simultaneously expressed the dCK mutants and a cell surface-expressed marker, cytoplasmic-tail-truncated version of the human CD19 molecule, from the same mRNA transcript by use of an internal ribosome entry site (IRES) element.[30] We transduced Jurkat and Molt-4 T cell lymphoma cell lines along with the U87mg glioblastoma–astrocytoma cell line at a multiplicity of infection of 20 with LVs engineering the expression of either the wild-type dCK (dCK.WT), dCK.R104M.D133A double-mutant (dCK.DM), dCK.R104M.D133A.S74E triple-mutant (dCK.DM.S74E), or the enhanced green fluorescent protein (eGFP). Marked overexpression of the dCK proteins in transduced Jurkat cells was confirmed by western blotting with an anti-dCK monoclonal antibody, which detected the expected dCK band of ~31 kDa (**Figure 1b**). Expression levels of wild-type dCK in nontransduced Jurkat cells were below the detection limit in this experiment.

To confirm the feasibility of immunoaffinity enrichment of transduced cells based on huCD19Δ marker expression and to ensure all cells further used in this study expressed the dCK CFC element, we isolated transduced Jurkat, Molt-4, and U87mg cells by fluorescence-activated cell sorting (FACS). The resulting populations were of 96–99% purity (**Figure 1c–e**). LV-eGFP-transduced U87mg cells were also successfully sorted to above 98% purity by FACS (data not shown). Importantly, we have not observed significant differences in cell proliferation rates between transduced cells and controls (data not shown). To confirm the genetic and expressional stability of our transduced Jurkat cell populations, the average copy number of integrated provirus was assessed by quantitative real-time PCR (Q-PCR). We found that all of our enriched long-term-cultured Jurkat cells harbored an average of three copies of integrated provirus per genome (**Figure 1f**).

Determination of intracellular accumulation of activated BVdU metabolites

To confirm the functionality of the dCK mutants, we assessed the accumulation of phosphorylated forms of BVdU by high-performance liquid chromatography analyses of cell extracts of transduced Jurkat cells following prodrug treatment. BVdU-treated cells that expressed the thymidine-activating dCK.DM or dCK.DM.S74E mutants demonstrated a significant accumulation of intracellular BVdU monophosphate, which was further phosphorylated by cellular kinases into BVdU-diphosphate and BVdU-triphosphate forms (**Figure 1g**). Importantly, we did not observe accumulation of BVdU monophosphate in nontransduced controls or cells overexpressing wild-type dCK, consistent with the inability of wild-type dCK to phosphorylate thymidine-based NAs.[24] Significant accumulation of BVdU-diphosphate and BVdU-triphosphate metabolites during this short 12-hour treatment indicated that we successfully overcame the rate-limiting step for BVdU activation in cells expressing the dCK.DM.S74E CFC element.

Sensitivity of human cell lines to BVdU and LdT prodrugs *in vitro*

Transduced and enriched polyclonal cultures of Jurkat, Molt-4, and U87mg cells were cultured in the presence of increasing concentrations of BVdU (**Figure 2a,c,e**) or LdT (**Figure 2b,d,f**) for a period of 5 days, after which cell viability was determined. Cells expressing the thymidine-activating dCK.DM and dCK.DM.S74E

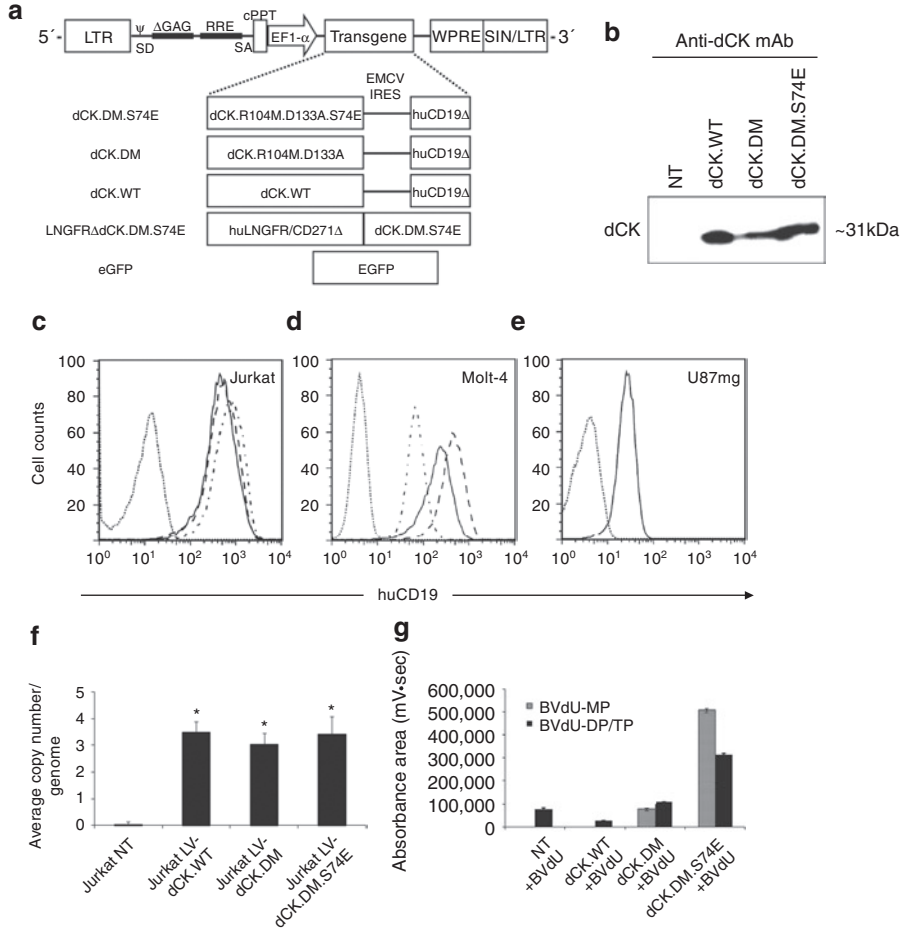

Figure 1 Characterization of lentiviral vector (LV)-driven dCK variant expression and prodrug activation *in vitro*. (**a**) Diagrammatic representation of LV expression constructs used in these studies. The transcription of the expression cassettes is driven off the elongation factor 1-α (EF1-α) promoter. The deoxyCytidine Kinase (dCK)-encoding vectors carry a bicistronic cassette, with the translation of the second cDNA, cytoplasmic tail-truncated human CD19 (huCD19Δ) marker, driven by the internal ribosomal entry site (IRES) derived from the encephalomyocarditis virus (EMCV). Ψ, human immunodeficiency virus packaging signal; cPPT, central polypurine tract; EGFP, enhanced green fluorescent protein; LNGFRΔ, cytoplasmic tail-truncated low-affinity nerve growth factor receptor; LTR, long-terminal repeat; RRE, rev response element; SA, splice acceptor; SD, splice donor; SIN, self-inactivating LTR; WPRE, woodchuck hepatitis virus post-transcriptional regulatory element. (**b**) Detection of overexpressed dCK enzyme by Western blotting of lysates from transduced Jurkat cells. Next, (**c**) Jurkat, (**d**) Molt-4, and (**e**) U87mg cells transduced with different LV/dCK constructs and sorted by fluorescence-activated cell sorting (FACS) were analyzed by flow cytometry for human CD19 expression (dotted line, nontransduced control cells; alternating dash/dot line, dCK.WT; dashed line, dCK.DM; solid line, dCK.DM.S74E). (**f**) Average provirus copy numbers in sorted populations of transduced Jurkat cells were quantified by WPRE-based quantitative-PCR (Q-PCR) and standardized against a cell line known to express a single proviral copy (error bars represent SE of the mean; $n = 3$; *indicates statistically significant difference, $P < 0.005$). (**g**) Lysates of transduced and nontransduced control Jurkat cells treated with 10 µmol/l bromovinyl-deoxyuridine (BVdU) for 12 hours were analyzed by high-performance liquid chromatography (HPLC) for intracellular accumulation of phosphorylated BVdU metabolites, immediate dCK product BVdU-monophosphate (BVdU-MP), BVdU-diphosphate and- triphosphate (BVdU-DP/TP) (error bars represent SD; $n = 3$; *indicates statistically significant difference, $P < 0.005$).

mutants demonstrated significantly increased sensitivity to both prodrugs. Underlining the high selectivity of the system, no loss of viability was observed in treated cultures of nontransduced controls or controls overexpressing wild-type dCK, with only limited toxicity in Jurkat and Molt-4 control cells treated with the highest, millimolar concentration of BVdU. U87mg and Jurkat cells expressing dCK.DM and dCK.DM.S74E were more sensitive to BVdU (EC_{50} of 0.3 µmol/l and 210 µmol/l for dCK.DM.S74E, respectively) than Molt-4 cells (EC_{50} of 62 µmol/l for dCK.DM.S74E), with complete cell killing at 100 µmol/l of BVdU as confirmed by trypan blue exclusion staining (data not shown). U87 and Jurkat cells expressing dCK.DM.S74E were similarly sensitive to LdT (EC_{50} of 210 µmol/l and 230 µmol/l, respectively), and were also more sensitive to LdT than Molt-4 cells (EC_{50} of 1 mmol/l). Jurkat and Molt-4 cells were also sensitive to LdU (EC_{50} of 30 µmol/l and 230 µmol/l, respectively, data not shown), but this prodrug is somewhat toxic to wild-type cells at high concentrations owing to the substrate promiscuity of wild-type dCK.

Identification of mechanisms of cell killing induced by BVdU-activation

Since BVdU has proven to be most effective for dCK-mediated CFCGT in these target cell populations, we investigated its underlying mechanisms of cell killing in depth. As evidenced by a significant increase in Annexin-V staining of Jurkat cells expressing

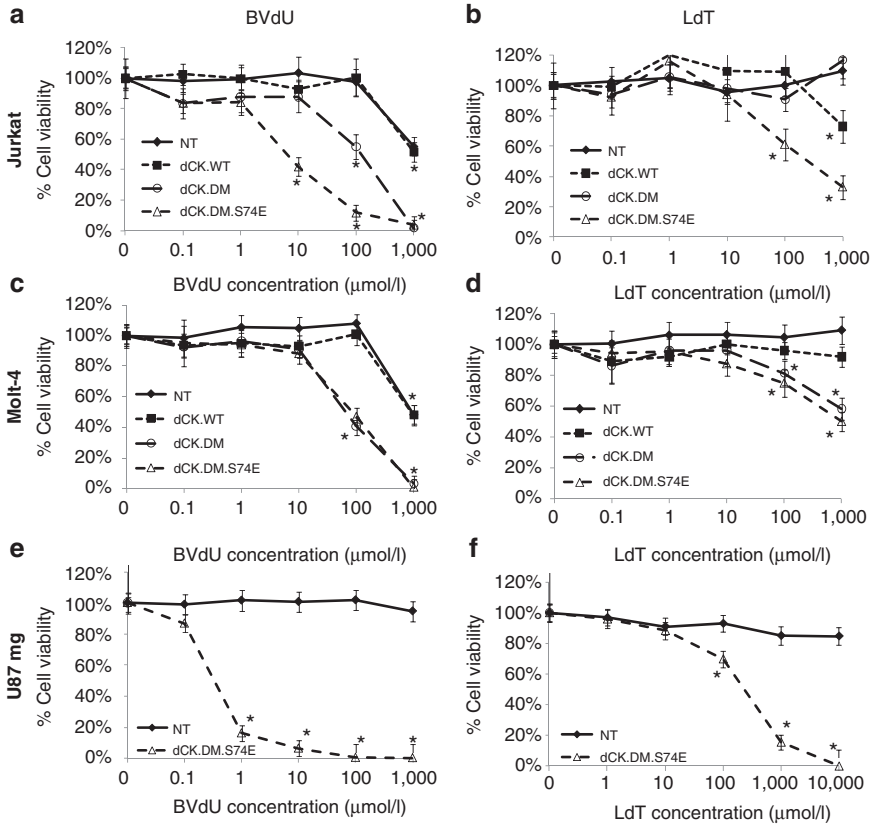

Figure 2 Sensitivity of deoxyCytidine Kinase (dCK)-transduced cells to prodrug treatment *in vitro*. Transduced and fluorescence-activated cell sorting (FACS)-enriched (**a**,**b**) Jurkat, (**c**,**d**) Molt-4, and (**e**,**f**) U87mg cells were treated with increasing concentrations of two thymidine-based nucleoside analogues, 0.1 μmol/l–1 mmol/l bromovinyl-deoxyuridine (BVdU) (**a**,**c**,**e**) and 0.1 μmol/l-10 mmol/l L-deoxythymidine (LdT) (**b**,**d**,**f**), in culture over a period of 5 days. After 5 days, viability was assessed by the MTS assay. Corresponding mean viability is plotted for each experiment. Cells were either nontransduced (closed diamonds), or transduced with either dCK.WT (closed squares), dCK.DM (open circles), or dCK.DM.S74E (open triangles). Data shown for each group were normalized to corresponding nontreated controls (error bars represent SE of the mean; each analysis was performed at least in triplicate; *indicates statistically significant difference compared to nontreated control, $P < 0.01$).

dCK.DM.S74E following BVdU-treatment for 5 days, we confirmed that BVdU activation induced cell death by apoptosis (**Figure 3a**). We further observed loss of mitochondrial inner membrane potential in cells expressing dCK.DM.S74E and treated with BVdU (**Figure 3b**).

BVdU-monophosphate is a competitive inhibitor of thymidylate synthase (TS) (K_i of 4.5 μmol/l).[31] Since TS inhibition in cells is known to induce cell proliferation arrest and caspase-dependent apoptosis, at least in part via the mitochondrial pathway,[32] we wanted to assess if TS inhibition by BVdU activation contributed to the cell killing observed in our hands. Indeed, the addition of exogenous thymidine (dThd) partially rescued cells from BVdU-mediated cell killing (**Figure 3c**). To evaluate BVdU-mediated cell killing of nondividing cells, CFSE-labeled cells were treated with a cell cycle progression inhibitor, nocodazole, and cultured in the presence or absence of 100 μmol/l BVdU. The apoptotic index of the $CFSE^{high}$ cell-cycle progression-inhibited cell population increased approximately twofold in the BVdU-treated group compared to untreated controls (**Figure 3d**). This increase in apoptosis was largely rescued by exogenous thymidine (**Figure 3d**). To assess BVdU-mediated cell killing in naturally nondividing cell populations, we transduced and enriched primary human T cells, activated them with anti-CD3/CD28 beads and interleukin (IL)-2, and then removed stimulation after 1 week to derive cell cycle-arrested T cells. In cell cultures that had stimulation removed, >95% of cells arrested in the G_0/G_1 phase of the cell cycle (**Supplementary Figure S2** and Table in **Figure 3e**). Importantly, the populations derived could be reactivated by addition of anti-CD3/CD28 beads and IL-2 back into the cell culture media (data not shown); thereby they mimic quiescent-state T cells that have the potential to cause GvHD. As shown in **Figure 3e**, stimulation-withdrawn, G_0/G_1-arrested T cells were still selectively killed by treatment with 100 μmol/l BVdU (**Figure 3e**), albeit to a lesser extent than activated, rapidly dividing T cells (**Figure 5c**, below). Taken together, these findings suggest that dCK-mediated activation of BVdU can drive cell killing of nondividing cells by apoptosis.

Tumor formation is repressed by dCK-based CFCGT *in vivo* in a xenogeneic murine model

To assess the efficiency of dCK-based cell killing *in vivo*, we established U87mg-derived subcutaneous tumors in Non-Obese/Diabetic Severe Combined Immunodeficient (NOD/SCID) mice. Long-term growth of tumors derived from transduced U87mg cells expressing the thymidine-activating dCK.DM.S74E, but not from eGFP-expressing control cells, was efficiently inhibited by a

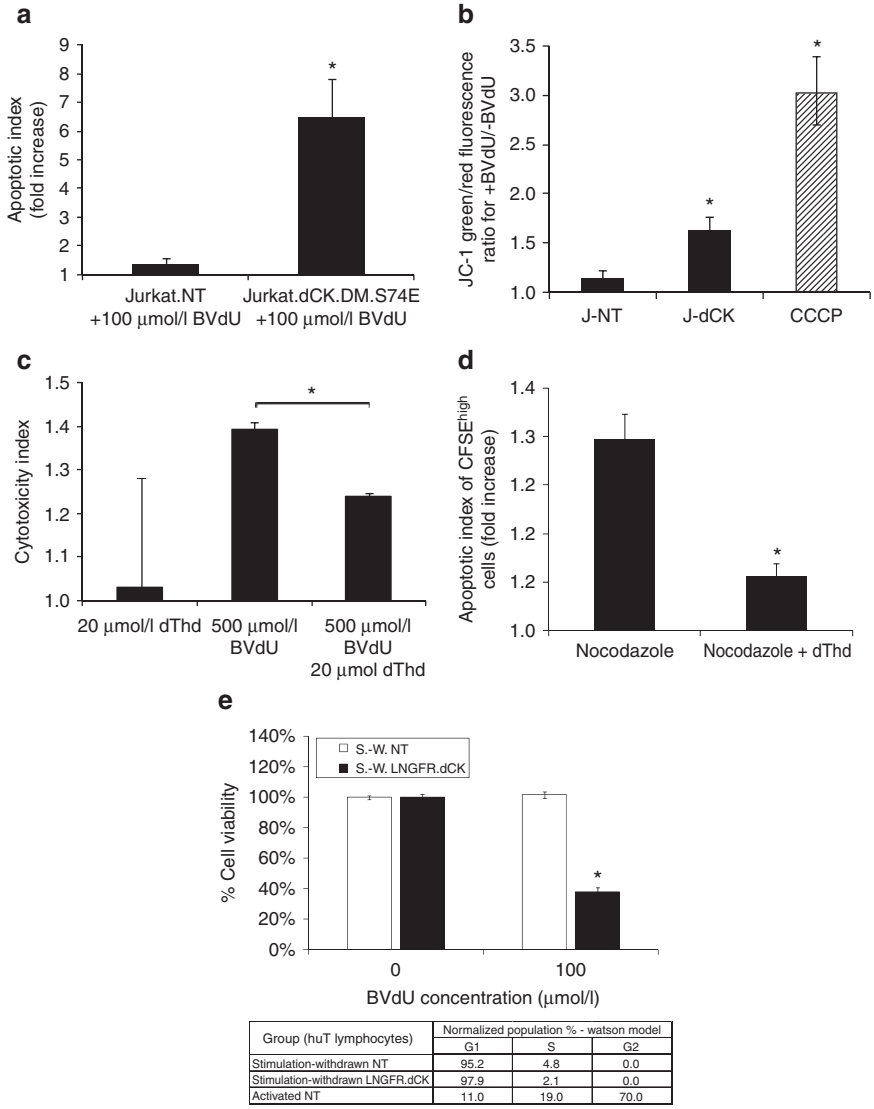

Group (huT lymphocytes)	Normalized population % - watson model		
	G1	S	G2
Stimulation-withdrawn NT	95.2	4.8	0.0
Stimulation-withdrawn LNGFR.dCK	97.9	2.1	0.0
Activated NT	11.0	19.0	70.0

Figure 3 Mechanisms of cell killing by activated bromovinyl-deoxyuridine (BVdU) in Jurkat cells expressing thymidine-activating deoxy-Cytidine Kinase (dCK). (**a**) Jurkat cells-expressing dCK.DM.S74E demonstrate a significant increase in the induction of apoptosis as measured by Annexin-V staining following 5 day treatment with 100 µmol/l BVdU (apoptotic index measures the fold increase in Annexin-V positive cells in BVdU-treated cells over untreated control). (**b**) Loss of mitochondrial inner membrane potential in Jurkat cells transduced with LV-dCK.DM.S74E and cultured in the presence or absence of 100 µmol/l BVdU for 48 hours (J-NT, nontransduced; J-dCK, dCK.DM.S74E-transduced; CCCP, 50 µmol/l carbonyl cyanide 3-chlorophenylhydrazone mitochondrial membrane potential disrupter). Increase in the ratio of green to red fluorescence of the JC-1 dye correlates with mitochondria disruption (error bars represent SD; data acquired in duplicate; *indicates statistically significant difference compared to nontransduced controls, $P < 0.05$). (**c**) Molt-4 cells transduced with dCK.DM.S74E and nontransduced controls were cultured in the presence or absence of 20 µmol/l dThd, 500 µmol/l BVdU, or both, for a period of 2 days. Viability was assessed by the MTS assay. Percent cell killing was calculated and normalized to nontreated controls. Cytotoxic index was calculated as the ratio of percent cell killing in dCK.DM.S74E-transduced cells to percent cell killing in nontransduced control cells for each treatment group (error bars represent SE of the mean; each analysis was performed in triplicate; *indicates statistically significant difference, $P < 0.005$). (**d**) Molt-4 cells transduced with dCK.DM.S74E and nontransduced controls were labeled with 10 µmol/l CFSE and cultured in the presence or absence of 100 µmol/l BVdU, and in the presence or absence of 0.1 µg/ml nocodazole, 20 µmol/l dThd, or both for 4 days. Induction of apoptosis in $CFSE^{high}$ nondividing cells was assessed by Annexin V staining. (Apoptotic index measures the fold increase in Annexin-V positive cells in BVdU-treated cells over untreated control. Error bars represent SD; data was acquired in duplicate; *indicates statistically significant differences between groups, $P < 0.05$). (**e**) Human T cells transduced with LNGFRΔ.dCK.DM.S74E vector and non-transduced controls were cultured with anti-CD3/CD28 beads and IL-2 stimulation removed (stimulation-withdrawn (S.-W.) cells). Cell-cycle distribution was assessed by propidium iodide staining of fixed cells, and analyzed by flow cytometry, with the results tabulated. Cell viability following a 4-day exposure of the cells to 100 µmol/l BVdU was assessed by the MTS assay. (Error bars represent SE; data acquired in quadruplicate; *indicates statistically significant differences between BVdU-treated and untreated groups, $P < 0.01$).

3-week treatment with 60 mg/kg/day BVdU injected intraperitoneally (**Figure 4a**). Palpable tumors were first detected in control mice at about 4 weeks (data not shown). After a long-term follow up of 12 weeks, only 4 out of the 11 mice (36%) in the U87mg-dCK.DM.S74E BVdU-treated group developed sizable tumors, compared to 100% of the mice in all the other groups ($n = 7–10$). Dissociated tumor cells from the U87mg-dCK.DM.S74E BVdU-treated group, analyzed by flow cytometry, showed either no expression or a

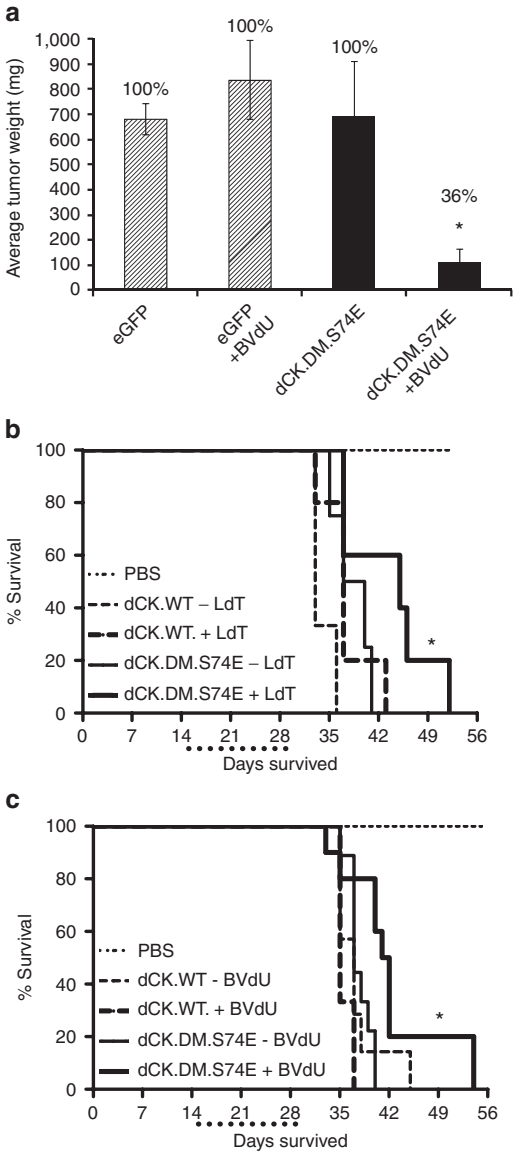

Figure 4 U87mg and Molt-4 cells transduced with the thymidine-activating mutant of deoxyCytidine Kinase (dCK) are sensitive to prodrug-mediated cell killing *in vivo* in tumor and leukemia models of cancer. (**a**) Subcutaneous tumors in NOD/SCID mice formed by U87mg cells transduced with dCK.DM.S74E but not control eGFP-transduced cells were efficiently eradicated *in vivo* by treatment with bromovinyl-deoxyuridine (BVdU) (eGFP, U87mg cells transduced with LV-eGFP; dCK.DM.S74E, U87mg cells transduced with LV-dCK.DM.S74E; +BVdU, treated with 60 mg/kg/day of BVdU for 21 days). (Error bars represent SE of the mean; percentages above the bars represent proportion of mice that had measurable tumors; n = 7–11 for treatment groups and n = 3 for PBS controls; *indicates statistically significant difference, P<0.005). (**b,c**) Kaplan-Meier survival curves of mice with Molt-4-derived leukemias. Aggressive T cell leukemia was induced in pre-conditioned NOD/SCID animals by intravenous tail vein administration of human Molt-4 cells (dCK.WT, Molt-4 cells transduced with LV-dCK.WT; dCK.DM.S74E, Molt-4 cell transduced with LV-dCK.DM.S74E; PBS, PBS-injected control animals; +LdT, treated with 50 mg/kg/day of L-deoxythymidine (LdT); +BVdU, treated with 50 mg/kg/day of BVdU; dotted line below x-axis underlines the drug treatment window). Survival of mice with established leukemias derived from Molt-4 cells-expressing dCK.DM.S74E was increased with LdT (**b**) or BVdU (**c**) treatments (median survival increase of 1 week) administered for 14 days starting day 15 after cell injection (n = 3–10; *indicates statistically significant difference compared to control, P < 0.05). LV, lentiviral vector.

marked reduction of huCD19Δ levels (data not shown), suggesting that populations of nontransduced cells or cells expressing very low levels of dCK.DM.S74E may have been preferentially amplified in that case.

CFCGT based on a thymidine-activating dCK mutant increased survival in a stringent model of T cell leukemia

To test the limits of dCK-based CFCGT, we employed a model of aggressive xenogeneic T cell leukemia in NOD/SCID animals. Tail-vein injections of Molt-4 cells resulted in a disseminated leukemia in 100% of injected animals with a median survival of ~5 weeks (**Figure 4b,c**). A 2-week treatment of animals with established leukemias derived from dCK.DM.S74E-transduced Molt-4 cells with 50 mg/kg/day of BVdU (**Figure 4b**) or LdT (**Figure 4c**) significantly increased median survival by 1 week, compared to untreated controls. No survival increase was observed in mice injected with Molt-4 cells overexpressing wild-type dCK (**Figure 4b,c**). Since the enriched cell populations were only ~96% positive for marker expression, we expected some selective amplification of residual, nontransduced cell populations or cells expressing low levels of dCK.DM.S74E. Indeed, analyses of internal tumors collected from several euthanized BVdU-treated animals showed a marked presence of nontransduced cells or huCD19Δ^{low} cells that ranged from 5 to 90%.

Effective CFCGT based on a truncated LNGFR-dCK mutant fusion in primary human T cells

We engineered and constructed the LNGFRΔ-dCK.DM.S74E direct fusion for applications involving cells that did not express high levels of our truncated huCD19, such as primary human T cells. Such a fusion also combines the cell marking and suicide functions into a single unit, allowing constructs of a bicistronic nature to be generated that may have different therapeutic foci. To ensure that the LNGFR-dCK fusion was stably expressed, we first transduced Jurkat cells with the LV engineering the expression of the LNGFRΔ-dCK.DM.S74E fusion and analyzed cell lysates by Western blotting (**Figure 5a**). Probing with both dCK- and LNGFR-directed antibodies yielded bands of the expected size. No bands of reduced apparent molecular weight were observed, suggesting that the fusion construct is proteolytically stable. Primary human T cells transduced with a LV engineering expression of the LNGFRΔ-dCK.DM.S74E fusion could be enriched by magnetic cell sorting to >99% purity based on the cell surface component of the fusion (**Figure 5b**). No significant changes in CD4/CD8 ratios following transduction, or changes in the ability of the transduced T cells to produce IFN-γ or IL-2 upon stimulation were observed (**Supplementary Figure S1**). Transduced human primary T cells, cultured in the presence of increasing concentrations of BVdU (**Figure 5c**) or LdT (**Figure 5d**) for 5 days, could be rapidly and selectively killed *in vitro* with an EC_{50} of ~2.5 µmol/l and ~350 µmol/l, for BVdU and LdT, respectively, with no significant toxicity to nontransduced cell controls at these prodrug concentrations. Finally, LNGFRΔ-dCK.DM.S74E-transduced primary T cells infused into NOD/SCID mice engrafted, and could be selectively and efficiently cleared from circulation with BVdU treatment (**Figure 5e**).

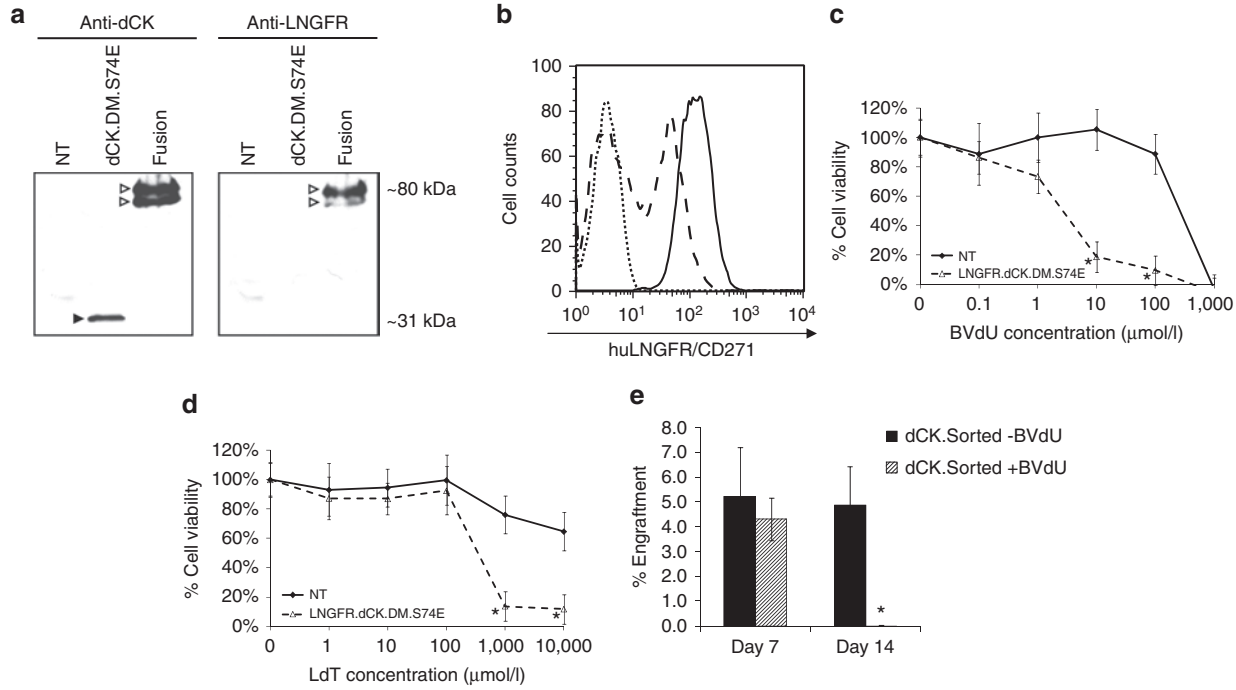

Figure 5 Primary human T lymphocytes transduced with the LNGFR-deoxyCytidine Kinase (dCK) fusion are sensitive to prodrug-mediated cell killing *in vitro*. (**a**) Cell lysates from Jurkat cells transduced with LVs engineering the expression of either the dCK.DM.S74E or the LNGFRΔ-dCK.DM.S74E were probed by western blotting for the expression of dCK (left panel) and LNGFR (right panel). (**b**) Nontransduced (dotted line) and LNGFRΔ-dCK.DM.S74E-transduced human T cells were analyzed by flow cytometry for the expression of huLNGFR, before (dashed line) and after (solid line) magnetic enrichment. LNGFRΔ-dCK.DM.S74E-transduced (dashed line) and nontransduced (solid line) human T cells were treated or not with increasing concentrations of (**c**) bromovinyl-deoxyuridine (BVdU) or (**d**) L-deoxythymidine (LdT) in culture over a period of 5 days. Viability was then assessed by the MTS assay. Corresponding mean viability is plotted for each experiment (error bars represent SE of the mean; each analysis was performed in triplicate; *indicates significant difference compared to control, $P < 0.01$). (**d**) 2×10^6 LNGFRΔ-dCK.DM.S74E-transduced human T cells were infused into pre-conditioned (day 0) NOD/SCID animals by intravenous tail vein administration (day 1). Animals were treated (shaded bars) with 50 mg/kg/day of BVdU on days 2, 3, 5, and 6, and then with 80 mg/kg/day for days 8–14, or left untreated (black bars). Percent engraftment of human T cells was measured by simultaneous staining of peripheral blood cells with antihuman CD45 and anti-LNGFR antibodies. ($n = 4$; *indicates statistically significant difference compared to untreated controls, $P < 0.05$).

DISCUSSION

CFCGT is potentially useful across a wide spectrum of therapeutic applications in cell and gene therapy, where it can provide a safety net against adverse outcomes. Such applications include, but are not limited to, managing GvHD in hematopoietic cell transplantation, improving safety of therapies based on embryonic stem cells and induced pluripotent stem cells, and safeguarding against oncogenic transformation that could be caused by integrating vectors in gene therapy. In addition, CFCGT can be used proactively in treating cancer, primarily relying on bystander effects in solid tumors (Neschadim, A, Wang, JCM, Lavie, A, and Medin, JA manuscript submitted, ref. 33). For successful application in the clinic, CFCGT must fulfill a number of criteria: it should be nonimmunogenic, have good prodrug-activation kinetics, and be able to affect different cell types, both dividing and nondividing. These criteria could be fulfilled by CFCGT based on the human thymidine-activating variant of dCK we describe herein, which provides several additional advantages as well. Firstly, the thymidine-activating variant of human dCK is predicted to have low immunogenicity in patients. Secondly, dCK, being a nucleoside kinase, permits effective imaging of genetically modified cells to assess both the progress of the therapy and the progress of CFCGT *in situ* by positron emission tomography using the ^{18}F-2′-fluoro-2′-deoxyarabinofuranosyl-5-ethyluracil radiotracer.[29] Thirdly, our novel dCK-based CFCGT permits the use of a range of thymidine-based (BVdU, LdT) and uridine-based (LdU) prodrugs with favorable pharmacokinetic properties and safety profiles. Finally, we have shown that dCK mutants can be directly fused to cell-surface markers, enforcing a 1:1 correlation in the expression of the marker and the cell fate control protein that would facilitate more complex vector construction involving other therapeutic sequences.

In this study, we have demonstrated the applicability of two clinically relevant prodrugs, BVdU and LdT, with our novel dCK-based CFCGT. We also reasoned that validating our dCK-based CFCGT efficiency using polyclonal cell populations (as opposed to single-cell-derived clonal populations) better reflected a level of heterogeneity expected following gene transfer into primary cells and is more relevant to clinical protocols. The two prodrugs, LdT and BVdU, have well-known toxicity profiles and are well-tolerated in patients.[34,35] Furthermore, both prodrugs possess good oral bioavailability that enables administration in the clinical setting.

BVdU is well-tolerated in mice at doses of 500–1,000 mg/kg/day administered over long periods of time.[35] Concentrations as high as 15 mg/kg/day have been successfully used in pediatric patients with no toxic side effects.[36] In a single 250 mg administration (for a 60–70 kg patient) Baba *et al.*[37] observed 1.2–2.2 μg/ml BVdU in the plasma at 1 hour post-administration. This dose is roughly

4 mg/kg and those concentrations translate into ~3.6–6.6 μmol/l. BVdU is well-absorbed if given orally and has been used in the clinic for over 30 years in some European countries for the treatment of herpes zoster. While active BVdU metabolites can inhibit DNA replication in dividing cells, BVdU is also effective against nondividing cells through the inhibition of TS, an essential enzyme in the *de novo* pathway of nucleotide synthesis.[38] Inhibition of TS by BVdUMP, a major intracellular metabolite of BVdU, induces cell proliferation arrest and caspase-dependent apoptosis via the mitochondrial pathway—at least in part.[32] In contrast, herpes simplex virus-derived thymidine kinase-mediated cell killing requires cell proliferation for the cytotoxic effect of ganciclovir, whereby ganciclovir triphosphate is incorporated into DNA of dividing cells causing DNA chain termination.

Like BVdU, LdT is well-tolerated in a range of animal species at doses of 2,000 mg/kg/day and higher.[39] Once monophosphorylated, LdT is efficiently phosphorylated further by nonstereospecific cellular kinases and inhibits cellular DNA polymerases.[40] Its plasma half-life in humans is 2.5–5 hours,[34] and it has been approved by the US Food and Drug Administration and the European Commission in 2006 for treatment of chronic hepatitis B.

Implementation of CFCGT that can activate multiple different prodrugs offers advantages for the clinic, permitting the selection of the most suitable prodrugs on an individual patient-by-patient basis. The different cell lines used in the current experiments, Jurkat, Molt-4, and U87mg, exhibited varying degrees of sensitivity to BVdU and LdT. In Jurkat cells, but not in the other cell lines tested, dCK.DM performed poorer than dCK.DM.S74E in response to BVdU (EC50 of 115 μmol/l and 6.5 μmol/l, respectively) and LdT (EC50 of >1 mmol/l and 230 μmol/l, respectively). One possibility is that the activity of dCK in this cell line could be under tight regulation by hypophosphorylation of its Ser74 residue, which has been documented in other studies.[41] Our S74E variant of dCK clearly overcomes this dependency. Of the three cell lines tested, U87mg cells showed an increased degree of sensitivity to BVdU, but not to LdT. The unusually high cytotoxicity in U87mg cells expressing dCK.DM.S74E following BVdU treatment may indicate the increased sensitivity of this cell line to TS inhibition. Importantly, we also demonstrated that primary human T cells could be efficiently transduced, enriched, and killed *in vitro* and *in vivo* with CFCGT based on the LNGFRΔ-dCK.DM.S74E fusion, highlighting the clinical utility of this vector construct for T cell-based therapies, in particular.

NOD/SCID models with human-origin malignancies represent an extreme scenario, whereby an aggressive tumor is growing in the absence of cancer immuno-editing present in immunocompetent hosts. We achieved efficient suppression of dCK.DM.S74E-expressing subcutaneous tumors in mice following BVdU treatment. Nevertheless, a few smaller tumors did manifest in some treated animals following the 12-week follow-up in this study. The tumors consisted of nontransduced cells or cells expressing lower transgene levels. However, this result is expected when polyclonal cell populations are used. Additionally, genetic and epigenetic instabilities of tumor cells have previously been identified as a serious limitation of suicide gene therapy in general, with either polyclonal or clonal cell populations.[42] Likewise, the preferential expansion of prodrug-nonresponsive cell populations is a limiting caveat of our stringent disseminated leukemia model. Additionally, all animals succumbed to malignancy, and this is likely due to cells migrating into areas of decreased accessibility of the prodrug, such as the CNS (since most animals had to be euthanized due to hind-limb paralysis). Other reasons could have contributed to this. Very high doses of BVdU and LdT are well-tolerated in mice. However, LdT and BVdU have poor aqueous solubility (~20 mg/ml and ~3 mg/ml, respectively), which does not permit the delivery by injection of much larger doses than those used in these current experiments. Other drug delivery schemas may need to be employed. Furthermore, there is some species variability in the plasma persistence of BVdU that could account for its poorer activity in mice. In one study, BVdU plasma half-life was measured in mice and in rats to be ~45 minutes, but in mice the prodrug was completely cleared after 6 hours, whereas in rats low levels of BVdU still persisted after that time.[43] These factors, however, should not be limiting in larger animal models and in human patients, where the plasma half-life of LdT and BVdU is >2 hours, and the terminal half-life of these drugs is much longer.[34,44]

Our studies demonstrate the broad applicability and utility of dCK-based CFCGT, which overcomes limitations of most current modalities. A new approach utilizing an inducible caspase-9 CFCGT has been recently evaluated in the clinic. That system enabled rapid clearance of gene-modified T cells and control of acute GvHD with complete remission for at least 12 months.[45] However, the clearance was still not optimized and re-expansion of gene-modified T cells that are less susceptible to prodrug-mediated killing was still observed.[45] Overall, the tunability of the threshold of inducible caspase-9 expression levels required for efficient cell killing and the basal toxicity of this construct, stemming from chemical dimerizer-independent activation of inducible caspase-9, need to be better defined in the context of long-term clinical follow-up and chronic GvHD.[46] Finally, the immunogenicity of the 20 amino acid-long 2A-like cleavable peptide of viral origin employed in that system, and largely retained with the cleaved caspase-9, has not been investigated yet.[47] We thus believe that novel CFCGT strategies based on fully human transgenes, such as the dCK-based system described here, provide for robust and tunable means of eradicating cells in case of adverse events. The ability to utilize multiple drugs, acting via complementary mechanisms, to eradicate GMCs, coupled with the ability to image the progress of the therapy by whole-body imaging *in situ*, are the major attractive features of this system.

MATERIALS AND METHODS

Construction of LV expression vectors and production of high-titer virus. Plasmids containing the cDNA for wild-type dCK and dCK.R104M.D133A were previously described.[24] Recombinant LV vectors for bicistronic expression of wild-type dCK and the R104M.D133A dCK double mutant (DM) were constructed by first subcloning the corresponding dCK cDNA into the pSV-IRES-huCD9Δ vector also described previously.[19] The resulting dCK-IRES-huCD19Δ cassette was then subcloned downstream of the EF1-α promoter into our HIV1-based recombinant LV expression plasmid, pHR′-cPPT-EF-WPRE-SIN, described previously.[48] The resulting pHR′-EF-dCK.DM-WPRE-SIN vector was then modified by QuikChange II XL Site-Directed Mutagenesis Kit (Stratagene, La Jolla, CA), following the manufacturer's instructions, to generate the pHR′-EF-dCK.DM.S74E-WPRE-SIN vector, coding for the R104M.D133A.S74E

dCK triple-mutant (DM.S74E).[24] The mutagenesis primers used were: S74E Forward 5′-CAAGATGAATTTGAGGAACTTACAATGGAGCAG AAAAATGGTGGGAATGTTC-3′ and S74E Reverse 5′-GAACATTCCC ACCATTTTTCTGCTCCATTGTAAGTTCCTCAAATTCATCTTG-3′. The LV vector encoding the eGFP cDNA, pHR′-EF-eGFP-WPRE-SIN, was described previously.[48] To construct an LNGFR-dCK fusion, the human LNGFR-encoding cDNA sequence was truncated in the intracellular region of the protein (after the Ser277 residue), and, through a cDNA encoding a flexible Ala-Gly-Gly-Ala-Ala-Gly spacer, fused directly in-frame to the cDNA of the dCK.DM.S74E mutant. The LNGFRΔ-dCK.DM.S74E sequence was codon optimized and synthesized to contain flanking 5′ *Asc*I and 3′ *BamH*I restriction sites by GenScript (Piscataway, NJ). The LNGFRΔ-dCK.DM.S74E cDNA was then subcloned into the pHR′-cPPT-EF-WPRE-SIN plasmid to give the final pHR′-cPPT-EF-LNGFR-ΔdCK. DM.S74E-WPRE-SIN construct. Fidelity of all constructs was confirmed by sequencing. VSV-g-pseudotyped LVs were generated by transient transfection of 293T cells (ATCC, Manassas, VA) with PEI (Sigma, Oakville, ON) using the three-plasmid system (pHR′ plasmid construct, packaging plasmid pCMVΔR8.91 packaging plasmid, and the pMD.G VSV-g expression plasmid). Viral supernatant was harvested, concentrated by ultracentrifugation, assessed for titer, and stored until use as described previously.[19]

Cell culture and transduction of cell lines. Human T cell lymphoma cell lines, Jurkat (ATCC) and Molt-4 (ATCC), were maintained in Roswell Park Memorial Institute 1640 media (RPMI-1640; Sigma) and supplemented with 10% fetal bovine serum (PAA, Toronto, ON), 100 U/ml penicillin, 100 µg/ml streptomycin, and 2 mmol/l glutamine (Invitrogen, Carlsbad, CA). Cells of the human glioblastoma-astrocytoma cell line, U87mg (ATCC), were maintained in Dulbecco's modified Eagle's medium (Sigma) supplemented as for RPMI-1640 above. Cells were infected with concentrated LVs at an approximate multiplicity of infection of 20 in the presence of 8 µg/ml of protamine sulfate (Sigma) over a culture period of 16 hours. Human primary T lymphocytes were expanded from Ficoll–Hypaque (Amersham, Piscataway, NJ) separations of peripheral blood mononuclear cells from peripheral blood of healthy volunteers. Briefly, peripheral blood mononuclear cells were maintained at 1×10^6 cells/ml in X-Vivo-20 (Lonza, Walkersville, MD) supplemented with 5% heat-inactivated human AB serum (Invitrogen). The T cells were activated using anti-CD3/CD28 beads (3×10^6 beads per peripheral blood mononuclear cells) and 20 IU/ml of recombinant human interleukin-2 (AbD Serotec, Raleigh, NC) in the presence of 1 µmol/l rapamycin (Sigma). T cells were infected at 48 hours of culture with concentrated LV at an approximate multiplicity of infection of 100.

Analysis of human CD19 and LNGFR expression along with enrichment of transduced cells. Expression of truncated human CD19 or LNGFR was assessed by flow cytometry on transduced cells at least 72 hours post-transduction. Transduced cells and nontransduced controls were immunostained at a 1:20 dilution with anti-CD19-PE, anti-CD19-APC, or anti-LNGFR-PE antibodies (BD Biosciences, San Jose, CA) and analyzed on a FACS Calibur flow cytometer (BD Biosciences) using the CellQuest software (BD Biosciences). To establish polyclonal transduced cell lines with high CD19 marker expression, cells were immunostained as above and sorted for the top 10% CD19 high-expressing cells on a BD FACS Aria (BD Biosciences). Following brief re-expansion in culture, cells were resorted again at least one or two times. Cells transduced with eGFP-coding LV were sorted similarly for high eGFP expression. Transduced primary T cells were enriched for high LNGFRΔ-dCK.DM.S74E expression by indirect magnetic cell sorting (MACS; Miltenyi Biotec, Auburn, CA), following the manufacturer's instructions. Briefly, cells were stained on ice with 1:20 diluted anti-LNGFR-PE antibody (BD Biosciences) and the supplied FcR-blocking reagent, then washed and stained on ice with rat anti-mouse IgG1 MicroBeads (Miltenyi Biotec). To obtain high-purity LNGFR$^+$ populations, labeled cells were passed through two sequential positive selection MS MACS separation columns (Miltenyi Biotec), following the manufacturer's instructions. To obtain cell cycle-arrested T cells, anti-CD3/CD28 beads and IL-2 stimulation was withdrawn following 1 week of culture.

Analysis of human CD4 and CD8 expression on transduced primary human T cells along with IFN-γ and IL-2 production in response to stimulation. Expression of human CD4 and CD8 was assessed by flow cytometry analyses of transduced cells at >72 hours post-transduction. Transduced cells and nontransduced controls were immunostained at a 1:20 dilution with anti-CD4-FITC and anti-CD8-APC antibodies (BD Biosciences) and analyzed on a FACS Calibur flow cytometer (BD Biosciences) using the CellQuest software (BD Biosciences). For stimulation with CD3/CD28 beads and/or IL-2, T cells were washed, plated at 10^6 cells/ml in the appropriate conditions, and cultured for 2 days. On day 3, stimulated T cells were fixed with 4% paraformaldehyde, permeabilized with 0.5% Triton-X100, blocked with phosphate-buffered saline (PBS) + 2.5% fetal bovine serum, and stained with a 1:20 dilution of either the antihuman IFN-γ or antihuman IL-2 antibody (BD Biosciences), and analyzed as above.

Analysis of dCK protein expression by western blotting. 5×10^6 dCK-transduced and nontransduced Jurkat cells were lysed by boiling in reducing Laemmli lysis buffer, resolved by a 10% SDS-PAGE, and transferred onto a polyvinylidene fluoride membrane (Millipore, Billerica, MA) by semidry transfer following the manufacturer's instructions. The membrane was blocked overnight at 4 °C (with shaking) in PBS-T (0.1% Tween-20 vol/vol in PBS) with 5% wt/vol nonfat dry milk. The membrane was stained for 4 hours at room temperature with an anti-dCK monoclonal antibody (Clone # 2243C2; Abcam, Cambridge, MA) diluted to 0.5 µg/ml in PBS-T with 5% wt/vol nonfat dry milk, washed with PBS-T, and then stained with secondary sheep anti-mouse immunoglobulin G antibody conjugated to horseradish peroxidase (Amersham) diluted 1:10,000 in PBS-T with 5% wt/vol nonfat dry milk for 4 hours at room temperature. Following washing with PBS-T, the membrane was then developed with Western Lightning Plus Enhanced Chemiluminescence Substrate (Perkin Elmer, Woodbridge, ON) and exposed onto Kodak X-Omat LS Film (Sigma). To probe the expression of LNGFR in cell lysates, Western blotting was performed as above with a primary anti-LNGFR-PE monoclonal antibody (Clone ME20.4; Cedarlane, Hornby, Ontario, Canada) diluted 1:200, and a secondary stabilized goat anti-rabbit immunoglobulin G (H+L) conjugated to horseradish peroxidase (Thermo Fischer Scientific, Nepean, ON) diluted 1:2,500.

Analysis of vector copy number by Q-PCR. Genomic DNA was isolated from transduced Jurkat cells and nontransduced control cells with the Gentra Puregene Blood Kit (Qiagen, Mississauga, ON) following the manufacturer's instructions. Q-PCR was carried out using a Rotor Gene RG300 system (Corbett Research, San Francisco, CA) as described previously.[49] Each DNA sample was tested in triplicate. Serial dilutions of DNA from a 293T cell line containing one copy of the WPRE sequence with nontransduced 293T cell line DNA were analyzed to establish a standard curve for interpolation of average copy number per genome for the unknown samples.

High-performance liquid chromatography analysis of intracellular BVdU metabolites. Transduced Jurkat cells and nontransduced control cells were cultured in the presence or absence of 10 µmol/l BVdU ((E)-5-(2-bromovinyl)-2′-deoxyuridine; Alfa Aesar, Ward Hill, MA) for 12 hours. 10^7 cells were washed and homogenized by sonication in 100 µl of 5% (wt/vol) trichloroacetic acid. The supernatant was collected after centrifugation at 10,000*g* for 15 minutes at 4 °C. trichloroacetic acid was removed by extraction with an equal volume of 20% tri-*n*-octylamine in pentane. The neutralized aqueous fraction was directly injected into the high-performance liquid chromatography apparatus (Waters, Milford, MA) in 20-µl aliquots for triplicate analyses. The method for the separation

and detection of BVdU metabolites was adopted from Ayisi *et al.*, with modifications.[50] Briefly, separation of BVdU metabolites was performed on a Symmetry C18 column (Waters) with a mobile phase composed of a linear methanol gradient rising from 25 to 50% (vol/vol) in 12 minutes, and the aqueous component containing 0.025 mol/l tetrabutylammonium bromide (Sigma) and 0.01 mol/l monobasic sodium phosphate (pH 5) at a flow rate of 1 ml/minute in a 33 minutes analysis cycle. The UV absorbance was monitored at 292 nm and 250 nm. Phosphorylated BVdU metabolite peaks were identified based on subtracted spectra for extracts from BVdU-treated and untreated cells expressing the thymidine-activating dCK.DM.S74E mutant or not, along with the expected elution order of the metabolites.[50]

Determination of BVdU, LdT, and LdU sensitivity of dCK-transduced cells in vitro. Transduced Jurkat, Molt-4, U87, and primary human T cells were plated at a density of 5×10^4 cells per well in 6-well tissue culture plates, and were cultured in the presence or absence of increasing concentrations of BVdU, LdT (β-L-2′-deoxythymidine (LdT), ChemGenes, Wilmington, MA), or LdU (β-L-2′-deoxyuridine (LdU); ChemGenes) for a period of 5 days. Fresh culture medium, with or without the drug, was added daily or every 2 days, as needed. Following treatment, cell viability was assessed using the Cell Titer 96 Aqueous One Solution Cell Proliferation Assay Kit (Promega, Madison, WI) following the manufacturer's instructions and scaled proportionately to a 6-well plate format. Following assay completion, 200 µl aliquots of culture supernatant were transferred in triplicate or quadruplicate onto a 96-well plate for absorbance measurements. Percent cell viability for each group was calculated by normalizing individual (blank-subtracted) absorbance values in drug-treated samples against the average absorbance of the nondrug-treated samples. For evaluation of apoptosis induction, cells were stained with Annexin-V conjugated to APC (BD Biosciences) following the manufacturer's instructions, propidium iodide was added to 1 µg/ml, and the cells were analyzed by flow cytometry as above. The apoptotic index was calculated based on the fold increase in the percentage of apoptotic (Annexin V-positive) cells in drug-treated over nondrug-treated groups.

Measurement of mitochondrial inner membrane potential following BVdU treatment. Changes to the mitochondrial membrane potential were assessed using the JC-1 Assay Kit for Flow Cytometry (Molecular Probes, Eugene, OR) following the manufacturer's instructions. Briefly, 2×10^5 transduced and nontransduced Jurkat cells were cultured in the presence or absence of 100 µmol/l BVdU for 48 hours. Following the treatment period, cells were incubated with 2 µmol/l JC-1 [5,5,6,6-tetrachloro-1,1,3,3-tetraethylbenzimidazolylcarbocyanine iodide] dye for 15 minutes at 37 °C, washed with warm PBS, and then analyzed by flow cytometry as above. 50 µmol/l carbonyl cyanide 3-chlorophenylhydrazone was used as the mitochondrial membrane potential disrupter in the positive control group. The ratio of mean fluorescence intensity of the green channel to red channel fluorescence was calculated for BVdU-treated and BVdU-untreated groups.

Measurement of cell killing due to inhibition of TS activity. Transduced and nontransduced Molt-4 cells were seeded at a density of 5×10^4 cells/well in a 6-well plate and treated (or not) with 500 µmol/l BVdU, in the presence or absence of 20 µmol/l exogenous thymidine (dThd; Sigma). Cell viability following 5 days of treatment was assessed with the Cell Titer 96 Aqueous One Kit (Promega) as above. The cytotoxicity index was calculated as the ratio of relative cell killing in the dCK.DM.S74E-transduced group to the nontransduced group.

Measurement of cell-cycle-independent cell killing in cell-cycle progression-inhibited cells. Molt-4 cells transduced with dCK.DM.S74E were labeled with 10 µmol/l CFSE (Invitrogen) following the manufacturer's instructions, and cultured in 6-well plates in the presence or absence of 100 µmol/l BVdU, and in the presence or absence of 0.1 µg/ml nocodazole, 20 µmol/l dThd, or both for 4 days. Induction of apoptosis in $CFSE^{high}$ cells was assessed by Annexin V staining as above in BVdU-treated and untreated groups, and expressed as an apoptotic index.

Subcutaneous tumor model in NOD/SCID mice. All experimental procedures involving animals were carried under a protocol approved by the Animal Care Committee of the University Health Network (Toronto, Ontario, Canada). NOD/SCID mice (male, 6–10 weeks old) were maintained at the Animal Resource Centre, Princess Margaret Hospital (Toronto, Ontario, Canada). Mice were injected into the right dorsal flank with 0.5×10^6 dCK-transduced or eGFP-transduced U87mg cells suspended in 200 µl of PBS on day 0. Animals in drug-treated groups received a dose of 60 mg/kg/day of BVdU intraperitoneally for 21 days starting day 1. The experimental groups were as follows: U87-dCK.DM.S74E +BVdU, U87-dCK.DM.S74E –BVdU, U87-eGFP +BVdU, and U87-eGFP –BVdU, PBS controls. Animals were euthanized at week 12, when the first animals reached a tumor-size endpoint (>1.5 cm^3). Tumors were extracted and weighed (with the exception of U87mg-eGFP animals that reached large tumor sizes quickly and were euthanized several weeks earlier). Cells from the tumors of the U87-dCK.DM.S74E +BVdU group were dispersed by individually passing each tumor through a 40 µ cell strainer and washing. These cells were further stained with anti-CD19-PE antibody and analyzed by flow cytometry as above.

Systemic leukemia model in NOD/SCID mice. NOD/SCID mice (male, 6–10 weeks old) were maintained as above. Mice were injected with 200 µg of anti-CD122 antibody (anti-IL-2 receptor β chain) from the TM-β1 hybridoma, described previously,[51] and sublethally irradiated at a 200 cGy dose on day 0. Cells ($4.5–5 \times 10^6$), suspended in PBS, were injected intravenously via the tail-vein on day 1. LdT or BVdU were injected intraperitoneally at a dose of 50 mg/kg/day for 14 days starting day 15. Experimental groups were as follows: Molt4-dCK.WT + drug, Molt4.dCK.WT – drug, Molt4.dCK.DM.S74E + drug, Molt4.dCk.DM.S74E – drug, PBS controls. Peripheral blood was collected weekly starting on day 15 of the experiment and analyzed for the presence of human $CD19^+$ cells by flow cytometry. Briefly, 50–200 µl of collected blood was treated with red blood cell lysis buffer (8.3 g/l ammonium chloride in 0.01 mol/l Tris–HCl; Sigma), blocked with normal rabbit serum (Sigma) and purified rat anti-mouse CD16/32 antibody (BD Biosciences), and then stained with antihuman CD19 antibodies as above. Mice were euthanized when they reached an experimental endpoint (limb paralysis, in the majority of cases).

Primary human T cell xenograft model in NOD/SCID mice. NOD/SCID mice (male, 6–10 weeks old) were maintained as above. Mice were injected with 200 µg of anti-CD122 antibody (anti-IL-2 receptor β chain) and sublethally irradiated at a 250 cGy dose on day 0. Sorted primary T cells (2×10^6), suspended in PBS, were injected intravenously via the tail-vein on day 1. BVdU was injected intraperitoneal at a dose of 50 mg/kg/day on days 2, 3, 5, and 6, and then escalated to 80 mg/kg/day on days 8–13. Experimental groups were as follows: huT.LNGFRΔ-dCK.DM.S74E +drug and huT.LNGFRΔ-dCK.DM.S74E –drug. Peripheral blood was collected weekly starting on day 1 of the experiment, and analyzed for the presence of human $CD45^+$ (and human LNGFR-positive) cells by flow cytometry. Briefly, 50–200 µl of collected blood was treated with red blood cell lysis buffer (8.3 g/l ammonium chloride in 0.01 mol/l Tris–HCl; Sigma), blocked with normal rabbit serum (Sigma) and purified rat anti-mouse CD16/32 antibody (BD Biosciences), and then stained with 1:20 diluted antihuman CD45-APC (BD Biosciences) and antihuman-LNGFR-PE antibodies. Mice were euthanized on day 14 and analyzed for presence of human T cells.

Statistical analyses. All experiments were performed in triplicate or quadruplicate (unless otherwise indicated), and repeated where applicable.

Data is presented as mean ± SE of the mean or SD, as per figure legends. Statistical analysis was performed by a two-tailed, two-sample Student's *t*-test, with *post-hoc* Bonferroni correction where multiple testing was applied. The *F*-test for variances was performed to determine the applicable Student's *t*-test. Statistical analyses of survival data were conducted using the log-rank (Mantel-Cox) and Gehan-Breslow-Wilcoxon tests (GraphPad Prism Version 5.03 for Windows; GraphPad Software, San Diego, CA).

SUPPLEMENTARY MATERIAL

Figure S1. Characterization of LNGFRΔ.dCK.DM.S74E-transduced primary human T cells.

Figure S2. Characterization of cell cycle in nontransduced and LV.LNGFRΔ.dCK.DM.S74E-transduced primary human T cells, in both stimulated and stimulation-withdrawn populations.

ACKNOWLEDGMENTS

The authors acknowledge Sean P. Devine (Department of Medical Biophysics, University of Toronto, Toronto, ON, Canada), Matthew Scaife (Department of Medical Biophysics, University of Toronto), and Orlay Lopez-Perez (University Health Network) for their assistance with methods development. Funding for A.N. was provided by the CIHR Training Program in Regenerative Medicine (TPRM). The authors declared no conflict of interest.

REFERENCES

1. Rezvani, AR and Storb, RF (2008). Separation of graft-vs.-tumor effects from graft-vs.-host disease in allogeneic hematopoietic cell transplantation. *J Autoimmun* **30**: 172–179.
2. Fraser, CJ, Hirsch, BA, Dayton, V, Creer, MH, Neglia, JP, Wagner, JE *et al.* (2005). First report of donor cell-derived acute leukemia as a complication of umbilical cord blood transplantation. *Blood* **106**: 4377–4380.
3. Amariglio, N, Hirshberg, A, Scheithauer, BW, Cohen, Y, Loewenthal, R, Trakhtenbrot, L *et al.* (2009). Donor-derived brain tumor following neural stem cell transplantation in an ataxia telangiectasia patient. *PLoS Med* **6**: e1000029.
4. Cooley, LD, Sears, DA, Udden, MM, Harrison, WR and Baker, KR (2000). Donor cell leukemia: report of a case occurring 11 years after allogeneic bone marrow transplantation and review of the literature. *Am J Hematol* **63**: 46–53.
5. Goring, DR and DuBow, MS (1985). A cytotoxic effect associated with 9-(1,3-dihydroxy-2-propoxymethyl)-guanine is observed during the selection for drug resistant human cells containing a single herpesvirus thymidine kinase gene. *Biochem Biophys Res Commun* **133**: 195–201.
6. Verzeletti, S, Bonini, C, Marktel, S, Nobili, N, Ciceri, F, Traversari, C *et al.* (1998). Herpes simplex virus thymidine kinase gene transfer for controlled graft-versus-host disease and graft-versus-leukemia: clinical follow-up and improved new vectors. *Hum Gene Ther* **9**: 2243–2251.
7. Deschamps, M, Mercier-Lethondal, P, Certoux, JM, Henry, C, Lioure, B, Pagneux, C *et al.* (2007). Deletions within the HSV-tk transgene in long-lasting circulating gene-modified T cells infused with a hematopoietic graft. *Blood* **110**: 3842–3852.
8. Garin, MI, Garrett, E, Tiberghien, P, Apperley, JF, Chalmers, D, Melo, JV *et al.* (2001). Molecular mechanism for ganciclovir resistance in human T lymphocytes transduced with retroviral vectors carrying the herpes simplex virus thymidine kinase gene. *Blood* **97**: 122–129.
9. Fehse, B, Ayuk, FA, Kröger, N, Fang, L, Kühlcke, K, Heinzelmann, M *et al.* (2004). Evidence for increased risk of secondary graft failure after *in vivo* depletion of suicide gene-modified T lymphocytes transplanted in conjunction with CD34+-enriched blood stem cells. *Blood* **104**: 3408–3409.
10. Ardiani, A, Sanchez-Bonilla, M and Black, ME (2010). Fusion enzymes containing HSV-1 thymidine kinase mutants and guanylate kinase enhance prodrug sensitivity *in vitro* and in vivo. *Cancer Gene Ther* **17**: 86–96.
11. Candice L, W, Django, S and Margaret E, B (2008). The role of herpes simplex virus-1 thymidine kinase alanine 168 in substrate specificity. *Open Biochem J* **2**: 60–66.
12. Willmon, CL, Krabbenhoft, E and Black, ME (2006). A guanylate kinase/HSV-1 thymidine kinase fusion protein enhances prodrug-mediated cell killing. *Gene Ther* **13**: 1309–1312.
13. Tiberghien, P, Ferrand, C, Lioure, B, Milpied, N, Angonin, R, Deconinck, E *et al.* (2001). Administration of herpes simplex-thymidine kinase-expressing donor T cells with a T-cell-depleted allogeneic marrow graft. *Blood* **97**: 63–72.
14. Bennour, E, Ferrand, C, Rémy-Martin, JP, Certoux, JM, Gorke, S, Qasim, W *et al.* (2008). Abnormal expression of only the CD34 part of a transgenic CD34/herpes simplex virus-thymidine kinase fusion protein is associated with ganciclovir resistance. *Hum Gene Ther* **19**: 699–709.
15. Bonini, C and Bordignon, C (1997). Potential and limitations of HSV-TK-transduced donor peripheral blood lymphocytes after allo-BMT. *Hematol Cell Ther* **39**: 273–274.
16. Riddell, SR, Elliott, M, Lewinsohn, DA, Gilbert, MJ, Wilson, L, Manley, SA *et al.* (1996). T-cell mediated rejection of gene-modified HIV-specific cytotoxic T lymphocytes in HIV-infected patients. *Nat Med* **2**: 216–223.
17. Berger, C, Flowers, ME, Warren, EH and Riddell, SR (2006). Analysis of transgene-specific immune responses that limit the *in vivo* persistence of adoptively transferred HSV-TK-modified donor T cells after allogeneic hematopoietic cell transplantation. *Blood* **107**: 2294–2302.
18. Noble, S and Faulds, D (1998). Ganciclovir. An update of its use in the prevention of cytomegalovirus infection and disease in transplant recipients. *Drugs* **56**: 115–146.
19. Sato, T, Neschadim, A, Konrad, M, Fowler, DH, Lavie, A and Medin, JA (2007). Engineered human tmpk/AZT as a novel enzyme/prodrug axis for suicide gene therapy. *Mol Ther* **15**: 962–970.
20. Sabini, E, Hazra, S, Ort, S, Konrad, M and Lavie, A (2008). Structural basis for substrate promiscuity of dCK. *J Mol Biol* **378**: 607–621.
21. Sabini, E, Hazra, S, Konrad, M, Burley, SK and Lavie, A (2007). Structural basis for activation of the therapeutic L-nucleoside analogs 3TC and troxacitabine by human deoxycytidine kinase. *Nucleic Acids Res* **35**: 186–192.
22. Sabini, E, Hazra, S, Konrad, M and Lavie, A (2007). Nonenantioselectivity property of human deoxycytidine kinase explained by structures of the enzyme in complex with L- and D-nucleosides. *J Med Chem* **50**: 3004–3014.
23. Sabini, E, Ort, S, Monnerjahn, C, Konrad, M and Lavie, A (2003). Structure of human dCK suggests strategies to improve anticancer and antiviral therapy. *Nat Struct Biol* **10**: 513–519.
24. Hazra, S, Sabini, E, Ort, S, Konrad, M and Lavie, A (2009). Extending thymidine kinase activity to the catalytic repertoire of human deoxycytidine kinase. *Biochemistry* **48**: 1256–1263.
25. Hazra, S, Ort, S, Konrad, M and Lavie, A (2010). Structural and kinetic characterization of human deoxycytidine kinase variants able to phosphorylate 5-substituted deoxycytidine and thymidine analogues. *Biochemistry* **49**: 6784–6790.
26. McSorley, T, Ort, S, Hazra, S, Lavie, A and Konrad, M (2008). Mimicking phosphorylation of Ser-74 on human deoxycytidine kinase selectively increases catalytic activity for dC and dC analogues. *FEBS Lett* **582**: 720–724.
27. Hazra, S, Szewczak, A, Ort, S, Konrad, M and Lavie, A (2011). Post-translational phosphorylation of serine 74 of human deoxycytidine kinase favors the enzyme adopting the open conformation making it competent for nucleoside binding and release. *Biochemistry* **50**: 2870–2880.
28. Toy, G, Austin, WR, Liao, HI, Cheng, D, Singh, A, Campbell, DO *et al.* (2010). Requirement for deoxycytidine kinase in T and B lymphocyte development. *Proc Natl Acad Sci USA* **107**: 5551–5556.
29. Likar, Y, Zurita, J, Dobrenkov, K, Shenker, L, Cai, S, Neschadim, A *et al.* (2010). A new pyrimidine-specific reporter gene: a mutated human deoxycytidine kinase suitable for PET during treatment with acycloguanosine-based cytotoxic drugs. *J Nucl Med* **51**: 1395–1403.
30. Gallardo, HF, Tan, C and Sadelain, M (1997). The internal ribosomal entry site of the encephalomyocarditis virus enables reliable coexpression of two transgenes in human primary T lymphocytes. *Gene Ther* **4**: 1115–1119.
31. Lackey, DB, Groziak, MP, Sergeeva, M, Beryt, M, Boyer, C, Stroud, RM *et al.* (2001). Enzyme-catalyzed therapeutic agent (ECTA) design: activation of the antitumor ECTA compound NB1011 by thymidylate synthase. *Biochem Pharmacol* **61**: 179–189.
32. Takezawa, K, Okamoto, I, Tsukioka, S, Uchida, J, Kiniwa, M, Fukuoka, M *et al.* (2010). Identification of thymidylate synthase as a potential therapeutic target for lung cancer. *Br J Cancer* **103**: 354–361.
33. Neschadim, A, McCart, JA, Keating, A and Medin, JA (2007). A roadmap to safe, efficient, and stable lentivirus-mediated gene therapy with hematopoietic cell transplantation. *Biol Blood Marrow Transplant* **13**: 1407–1416.
34. Lai, CL, Lim, SG, Brown, NA, Zhou, XJ, Lloyd, DM, Lee, YM *et al.* (2004). A dose-finding study of once-daily oral telbivudine in HBeAg-positive patients with chronic hepatitis B virus infection. *Hepatology* **40**: 719–726.
35. de Clercq, E, Degreef, H, Wildiers, J, de Jonge, G, Drochmans, A, Descamps, J *et al.* (1980). Oral (E)-5-(2-bromovinyl)-2′-deoxyuridine in severe herpes zoster. *Br Med J* **281**: 1178.
36. Benoit, Y, Laureys, G, Delbeke, MJ and De Clercq, E (1985). Oral BVDU treatment of varicella and zoster in children with cancer. *Eur J Pediatr* **143**: 198–202.
37. Baba, M, Shigeta, S and De Clercq, E (1987). Serum and urine concentrations of oral bromovinyldeoxyuridine in humans as monitored by a bioassay system based on varicella-zoster virus focus inhibition. *J Med Virol* **22**: 17–23.
38. Balzarini, J, De Clercq, E, Verbruggen, A, Ayusawa, D, Shimizu, K and Seno, T (1987). Thymidylate synthase is the principal target enzyme for the cytostatic activity of (E)-5-(2-bromovinyl)-2′-deoxyuridine against murine mammary carcinoma (FM3A) cells transformed with the herpes simplex virus type 1 or type 2 thymidine kinase gene. *Mol Pharmacol* **32**: 410–416.
39. Bridges, EG, Selden, JR and Luo, S (2008). Nonclinical safety profile of telbivudine, a novel potent antiviral agent for treatment of hepatitis B. *Antimicrob Agents Chemother* **52**: 2521–2528.
40. Focher, F, Maga, G, Bendiscioli, A, Capobianco, M, Colonna, F, Garbesi, A *et al.* (1995). Stereospecificity of human DNA polymerases alpha, beta, gamma, delta and epsilon, HIV-reverse transcriptase, HSV-1 DNA polymerase, calf thymus terminal transferase and Escherichia coli DNA polymerase I in recognizing D- and L-thymidine 5′-triphosphate as substrate. *Nucleic Acids Res* **23**: 2840–2847.
41. Smal, C, Vertommen, D, Bertrand, L, Rider, MH, van den Neste, E and Bontemps, F (2006). Identification of phosphorylation sites on human deoxycytidine kinase after overexpression in eucaryotic cells. *Nucleosides Nucleotides Nucleic Acids* **25**: 1141–1146.
42. Frank, O, Rudolph, C, Heberlein, C, von Neuhoff, N, Schröck, E, Schambach, A *et al.* (2004). Tumor cells escape suicide gene therapy by genetic and epigenetic instability. *Blood* **104**: 3543–3549.
43. Grignet-Debrus, C, Cool, V, Baudson, N, Degrève, B, Balzarini, J, De Leval, L *et al.* (2000). Comparative *in vitro* and *in vivo* cytotoxic activity of (E)-5-(2-bromovinyl)-2′-deoxyuridine (BVDU) and its arabinosyl derivative, (E)-5-(2-bromovinyl)-1-beta-D-arabinofuranosyluracil (BVaraU), against tumor cells expressing either the Varicella zoster or the Herpes simplex virus thymidine kinase. *Cancer Gene Ther* **7**: 215–223.
44. De Clercq, E (1986). Potential of bromovinyldeoxyuridine in anticancer chemotherapy. *Anticancer Res* **6**: 549–556.

45. Di Stasi, A, Tey, SK, Dotti, G, Fujita, Y, Kennedy-Nasser, A, Martinez, C *et al.* (2011). Inducible apoptosis as a safety switch for adoptive cell therapy. *N Engl J Med* **365**: 1673–1683.
46. Straathof, KC, Pulè, MA, Yotnda, P, Dotti, G, Vanin, EF, Brenner, MK *et al.* (2005). An inducible caspase 9 safety switch for T-cell therapy. *Blood* **105**: 4247–4254.
47. Tey, SK, Dotti, G, Rooney, CM, Heslop, HE and Brenner, MK (2007). Inducible caspase 9 suicide gene to improve the safety of allodepleted T cells after haploidentical stem cell transplantation. *Biol Blood Marrow Transplant* **13**: 913–924.
48. Yoshimitsu, M, Sato, T, Tao, K, Walia, JS, Rasaiah, VI, Sleep, GT *et al.* (2004). Bioluminescent imaging of a marking transgene and correction of Fabry mice by neonatal injection of recombinant lentiviral vectors. *Proc Natl Acad Sci USA* **101**: 16909–16914.
49. Walia, JS, Neschadim, A, Lopez-Perez, O, Alayoubi, A, Fan, X, Carpentier, S *et al.* (2011). Autologous transplantation of lentivector/acid ceramidase-transduced hematopoietic cells in nonhuman primates. *Hum Gene Ther* **22**: 679–687.
50. Ayisi, NK, De Clercq, E, Wall, RA, Hughes, H and Sacks, SL (1984). Metabolic fate of (E)-5-(2-bromovinyl)-2′-deoxyuridine in herpes simplex virus- and mock-infected cells. *Antimicrob Agents Chemother* **26**: 762–765.
51. McKenzie, JL, Gan, OI, Doedens, M and Dick, JE (2005). Human short-term repopulating stem cells are efficiently detected following intrafemoral transplantation into NOD/SCID recipients depleted of CD122+ cells. *Blood* **106**: 1259–1261.